White Rose Research Online

eprints@whiterose.ac.uk
https://eprints.whiterose.ac.uk
Universities of Leeds, Sheffield and York

Deposited via The University of Leeds.

White Rose Research Online URL for this paper:
https://eprints.whiterose.ac.uk/id/eprint/117213/

Version: Accepted Version

Article:
Lydon, JE, Gleeson, H and Jull, EIL (2017) The identification of the sign and strength of disclinations in the schlieren (nucleated domain) texture of the nematic phase, by optical microscopy. Liquid Crystals, 44 (12-13). pp. 1775-1786. ISSN: 0267-8292

https://doi.org/10.1080/02678292.2017.1336580

(c) 2017, Taylor & Francis. This is an Accepted Manuscript of an article published by Taylor & Francis in Liquid Crystals on 15 June 2017, available online: https://dx.doi.org/10.1080/02678292.2017.1336580

Reuse
Items deposited in White Rose Research Online are protected by copyright, with all rights reserved unless indicated otherwise. They may be downloaded and/or printed for private study, or other acts as permitted by national copyright laws. The publisher or other rights holders may allow further reproduction and re-use of the full text version. This is indicated by the licence information on the White Rose Research Online record for the item.

Takedown
If you consider content in White Rose Research Online to be in breach of UK law, please notify us by emailing eprints@whiterose.ac.uk including the URL of the record and the reason for the withdrawal request.

UNIVERSITY OF LEEDS
University of Sheffield
UNIVERSITY of York

The identification of the sign and strength of disclinations in the schlieren (nucleated domain) texture of the nematic phase, by optical microscopy.

Helen Gleeson[1], Ethan I, L. Jull[1] and John E. Lydon[2]

Il y a de certains dèfaults qui, bien mis en œuvre, brillent plus que la vertu même *
La Rochefoucauld

Abstract: The optical texture of the nematic phase, variously known as the *schlieren, structure à noyuax* or *nucleated domain texture*, was identified over a century ago as being an array of point singularities. When viewed between crossed polars, patterns of dark brushes radiate from each point nucleus. The *sign* and *strength* of each nucleus can be uniquely determined from the changes in the orientation of these brushes when either the sample or the crossed polars are rotated, from two formulae given by Chadrasekhar in 1977. However, these were given with little exemplification, and have been largely overlooked. Consequently the majority of the discussions given in current literature are either, incomplete and confusing, or in some cases, incorrect. Here we provide a detailed explanation of the textures and their behaviour as viewed with the most commonly used experimental geometry (i.e. with a rotating sample and stationary polars).

Key words Nematic Liquid Crystalline Phase, Schlieren, Structures à Noyeaux, Nucleated Domain textures, Disclinations, Polarising microscopy.

1 Introduction

1.1 The nucleated domain texture

This paper concerns the optical texture of nematic phases, identified over a hundred years ago, which is formed by rapid cooling of the isotropic liquid between a glass slide and cover slip with untreated surfaces [2]. It would appear that, on cooling, as the mesophase emerges from the isotropic melt, regions of the sample take up different alignments. Rather than spreading the initial disorder evenly throughout the volume of the sample, the lowest accessible energy minimum is for this disorder to be largely reduced to point and line singularities. Although this has been recognised since the earliest days of liquid crystal research, understanding the geometry and related optical properties of topological defects in mesophases and other condensed systems, is still of current interest - as witnessed by the 2016 Nobel Prize in Physics [3]).

The optical texture shown in Figure 1 is a consequence of this concentration of disorder around point and line disclinations. It is usually called the *schlieren* texture [2] but it is also known as the *structure à noyeau* or nucleated domain texture. When viewed between crossed polars, patterns of black brushes can be seen radiating from small points. Some of these 'nuclei' have two radiating dark brushes and others have four (nuclei with higher numbers are known, but are rarely encountered). Although the pattern of brushes changes continuously as the sample is rotated, the positions of the actual nuclei remain stationary. The nuclei are singularities in the director field. Various structures were postulated for them, based on studies using polarised light microscopy. These have been subsequently confirmed by independent approaches where the director field can be can be viewed directly, rather than inferred from the optics. These include the bubble technique (see Figure 2) [4].

---

* Footnote: This very appropriate quotation was used by de Gennes and Prost in the heading of Chapter 4 of [1].

1 School of Physics and Astronomy, The University of Leeds, Leeds LS2 9JT
2 Faculty of Biological Sciences, The University of Leeds, Leeds LS2 9JT

Figure 1 about here

Figure 1
The nucleated domain texture of a nematic phase - produced by rapid cooling of an isotropic sample, held between two glass slides, both with untreated surfaces – and viewed between crossed polars. Note the characteristic appearance of a mixture of two-brush and four-brush nuclei.

Figure 2 about here

Figure 2
Optical micrograph produced by the bubble-decoration technique, showing the director field pattern at a free surface of a nematic sample, viewed between crossed polars
Two point singularities are shown - the upper of strength +1 and the lower of strength -1.
Reproduced from Figure 4.4 [1p167], which had itself been reproduced from [4].

1.2 Point or line disclinations?

Since the samples are examined in projection, their appearance could arise from two kinds of molecular arrangement - either point disclinations (usually located at the top or bottom boundary surfaces of the sample), or line disclinations running through the sample, normal to the plane of the surfaces, as sketched in Figure 3. In practice, it appears that both types occur [1, p183]. They can usually be distinguished by the test described by Friedel and Kleman, where the cover slip is displaced sideways [5,6]. The appearance of a point disclination will not change significantly. However, a line disclination will be tilted out of the vertical, and, when seen in projection, the original point will be stretched into a short line.

Figure 3 about here

Figure 3 Line and point disclinations

(a)The director field pattern for an s = +1/2 disclination line running vertically through the sample. The molecules lie parallel to the horizontal plane (as indicated by the flat arrow). The family of curved surfaces indicate the pattern of molecular alignment - they are not intended to imply that the structure is layered.
(b) The director field pattern for an s = +1 point nucleus at the upper surface of the sample.

In texts describing the optical microscopy of mesophase textures, the nuclei are usually treated as if they were line disclinations seen end-on. This may not be a valid assumption. According to de Gennes, two-brush nuclei are always associated with a line disclination, whereas four-brush nuclei usually (but not invariably) arise from point disclinations, [1p28]. However, since both types have more or less identical appearances when viewed in projection, the uncertainty of whether a nucleus is a point or a line viewed end-on does not affect the discussion given in this paper.

1.3 Signs and strengths of disclinations

The four commonly-observed director-field patterns around the nuclei are sketched in Figure 4. They can be classified in terms of their strength, s and the sign, +/-. The way in which these parameters are defined is illustrated for s = +/- 1 in Figure 5. The strength of a nucleus is defined as the number of times the local director (shown as blue arrows) rotates whilst making a circuit around the nucleus. If s = ± 1, the local director rotates by an angle of 2π during a circuit. If s = ±½, the local director only rotates by π. The ± sign indicates whether the sense of the rotation (i.e. clockwise or anti-clockwise) for the circuit is the same as, or opposite to, that of the rotation of the local director.

Figure 4 about here

Figure 4
The director field patterns of the four most commonly observed nuclei in the nematic nucleated domain texture.

Figure 5 about here

Figure 5
Definition of the sign and strength of a nucleus – illustrated for the +1 and -1 cases. The strength, s of a nucleus is defined as the number of times the local director (shown as blue arrows) rotates whilst making a circuit around the nucleus. For the s = +1 case, the alignment of the local director, indicated by angle ω, makes one 360^o revolution, during a circuit. The positive sign indicates that the sense of rotation of the local director is the same as that of the circuit (i.e. clockwise). For the -1 nucleus, the local director also makes one rotation per circuit, but in the opposite sense, (anti-clockwise).

The signs and strengths of nuclei are not merely descriptive terminology. The values of s are useful when discussing the factors which determine changes in the nucleated domain texture. For example, because of the local bend, twist and splay distortions of the director field, there are attractive forces between nuclei of opposite signs and repulsive forces between those of like signs.

Often, particularly at temperatures close to the clearing point (where the viscosity of the phase is low), disclinations of opposite sign can be observed moving together and eventually coalescing, cancelling each other and disappearing. Alternatively, in other cases, two nuclei with the same sign can combine to form a new nucleus of a strength which is the sum of the original two values [7].

The nucleated domain structure can be regarded, as being a locked-in metastable state with the various forces and torques in a state of balance. Although it must have a higher free energy than a perfectly aligned sample, the available energy of thermal motion is not sufficient to allow the molecules to escape from their local free energy wells.

There is a kind of geometrical arithmetic operating where the numbers of positive and negative nuclei present in a sample tend to be equal, so that the sum of the strengths of all disclinations tends to be zero. Where new disclinations are created by mechanically disturbing the sample, they are usually created in pairs with opposite signs. In a recent paper, Dierking, Alexander and Yoemans have examined the dynamics of the mutual annihilation of linear $s = \pm 1$ pairs (both experimentally and in simulation [8]).

New disclinations can be introduced around foreign solid particles, by local melting and quenching of the mesophase. The recent work by Musevic and co-workers epitomises some of the elegant work that has been carried out in this area [9-11].

In an optical texture, where two adjacent nuclei are connected by brushes, these nuclei are of opposite sign. If we attempt to create a director field pattern which contains a group of +1 nuclei, as sketched in Figure 6, it is apparent that one cannot avoid creating a -1 nucleus between them.

Figure 6 about here

Figure 6
One cannot construct a stable director field composed solely of nuclei with positive signs. This sketch illustrates how four neighbouring +1 nuclei will create a -1 nucleus between them. In general the numerical sum of the strengths of the nuclei in a sample tends to be zero.

1.4 Radial lines

Prominent features of the director field patterns drawn in Figure 4 are what we shall term ‘radial lines’ – the parts of the patterns where the director field points towards the centre of the nucleus, dividing the pattern into a number of identical segments. The geometrical relationship which gives rise to these lines is described in Figure 7, using the $s = +1$ and $s = -½$ nuclei as examples.

Figure 7 about here

Figure 7
The creation of radial lines
The two large circles show the circuit around the nucleus, measured by the angle α. The small circles show the rotation of the director measured by the angle ω. In the case of s = +1, the angle ω is equal to the angle α at all positions on the circuit and every radius corresponds to a radial line in the director field, where the director points towards the centre of the nucleus. For the case of s = -½, the angle ω only matches the angle α (or $180^o + \alpha$) at three positions - where $\alpha = 0^o$, 120^o and 240^o - producing three radial lines. Figure (b) shows the situation where a 240^o journey around the circuit produces a 120^o rotation of the director in the opposite sense. In general, the number of radial lines of a nucleus is 2-2s.

1.5 The special case of s = +1

In general, the value of s uniquely determines the director field pattern around a nucleus. However the special case of s = +1 is the exception and here, the director field along the radius where $\alpha = 0^o$ is retained for all radii. This allows a sequence of structures ranging from radial to tangential patterns to be created, as shown in Figure 8. In this discussion we shall treat all +1 structures as radial. Apart from some curvature of the brushes for spiral cases like (e) where the director is inclined at an angle other than 0^o or 90^o to the radius, this will not affect the validity of any of the discussion in this paper. It is perhaps not surprising that spiral patterns are commonly observed for chiral nematic systems.

Figure 8 about here

Figure 8 The unique nature of the s = +1 nucleus
In general, changing the initial value of ω where $\alpha = 0^o$ merely causes a rotation of the whole director field pattern – and does not otherwise alter its appearance (as illustrated for s = +1/2, in Figures a, b and c). In this sketch, the values of ω when $\alpha = 0^o$ are drawn at 0^o, $+20^o$ and $+40^o$ respectively.
However, for the unique case of s = +1, all radii are identical and when the specimen is rotated between stationary crossed polars, the brush pattern remains stationary.
A further consequence is that the choice of initial value of ω produces different patterns, ranging from radial (d) to spiral (e) to tangential (f).

1.6 Half–integral nuclei

Figure 9 about here

Figure 9 Half-integral nuclei and the polarity of the nematic phase

The sketch (a) shows a hypothetical 'polar' nematic phase attempting to wrap itself around an s = +1/2 disclination. Note the unacceptable high-energy interface (indicated in red) created where molecules pointing to the left encounter molecules pointing to the right As shown in (b) this problem does not arise for a non-polar phase where equal numbers of molecules point in each direction along the director.

The sketches in Figure 9 show the problem encountered by a 'polar' nematic phase when forming an s =+1/2 disclination. The interface (indicated in red), where molecules pointing to the left encounter molecules pointing to the right would presumably be an unacceptable high-energy interface. The widespread occurrence of half-integral nuclei is taken to be proof that nematic phases are non-polar, and have equal numbers of molecules pointing in each direction along the director, as represented in (b).

2 Extinction brushes

Extinction brushes are regions of the sample observed between crossed polars, where the director is either parallel or perpendicular to the plane of polarization of the incident light. Nuclei with half-integral values form two bushes, whereas nuclei with strength ± 1 give four. In general the number of brushes is 4s.

The various patterns of brushes for nuclei with values of s from +2 to -2 are shown in Figure 10 Note that, although the director fields are very different, the brush patterns are the same for positive and negative values of s. An example of a rarely encountered 6 –fold brush pattern (given by disclinations with strength ± 3/2) is shown in Figure 11. The sign can be determined by observing the rotation of the brushes as the stage is rotated, as discussed below in section 4.

Figure 10 about here

Figure 10 The director field patterns and brush patterns for nuclei with s values from -2 to +2.

The various director field patterns around the nuclei are shown, with the brush patterns, observed between crossed polars, indicated by the darker shading. Of these, the four patterns shown at the top, ±½ and ±1, are the most common, and the lower four are rarely encountered.

Figure 11 about here

Figure 11 Optical micrograph of a nucleated domain texture of a nematic phase showing a rarely-observed six-brush pattern (produced by a nucleus of strength ±3/2).
Recorded by Ethan Jull.

As indicated in Figure 12, when the sample is rotated on the stage, the pattern of brushes does not fade and then reappear - the brushes retain their appearance but in general (as discussed below) they rotate around the central point of the nucleus. In one special case, where s = +1, shown in Figure 8 (and for one particular mode of operating the microscope), the brush pattern remains stationary. In all other cases the brushes rotate - in either the same sense as the rotation of the stage, or in the opposite sense. And, in general, the rate of rotation of the brush pattern is not the same as that of the stage.

Figure 12 about here

Figure 12 Sketch of the director field around an s = -1/2 nucleus, rotating between crossed polars, with the extinction brushes indicated. Note that the two-brush pattern occurs for all alignments of the sample.

3 Graphs of α against ω

3.1 Idealized director field patterns

In this discussion, we shall deal with the idealized structure of the nuclei as depicted in Figure 13, i.e. the structure near to the nuclear centre, where the director field pattern is not disturbed by the influence of neighbouring nuclei. Here all radii are lines of parallel alignment - and a circular orbit around a nucleus encounters a constant rate of elastic distortion of the mesophase.

Figure 13 about here

Figure 13 The idealised structure of a nucleus of the nucleated field texture (illustrated for an s = -½ nucleus). There are two geometric features: -

(a) The bend and splay distortions are constant around the circumference of a circle centred on the disclination.
(b) The local director field alignments are parallel at all points along a radius.

3.2 Relationship between the a/ω plot and the director field of the nuclei

Perhaps the reason why there has been so much confusion over the optical behaviour of the various types of nuclei is that the whole topic is littered with counter-intuitive features. Unexpected symmetries arise with no obvious reason - the three-fold symmetry of the s = -1/2 nucleus (and the 5-fold symmetry of the S = -3/2) being particularly puzzling at first sight. The symmetry of the brush patterns is not usually the same as that of the director field and furthermore, the way in which the orientation of the brush patterns changes as the samples are rotated, does not appear to fit into any immediately recognisable sequence.

Some insight into these three features is given by the graphs of α against ω. The case of s = + ½ is shown as an example, in Figure 14.

Figure 14 about here

Figure 14
The relationship between the α/ω plot and the director field pattern around a nucleus, (illustrated for the s = +1/2 case). Circulation around the nucleus by an angle α, corresponds to a horizontal sweep across the graph. The small blue squares represent the two alignments indicated by the double-headed blue arrow. The two lines on the graph indicate values of ω, and $\omega + 180^o$ (see Figure 9) for the alignment of the local director. In this and all subsequent α/ω plots, the grid lines are drawn at 90^o intervals for both angles.

Figure 15 about here

Figure 15 The single unique radial line of the s = +1/2 nucleus. The two solid lines on the α/ω graph indicate values of ω, and $\omega + 180^o$ (see Figure 7) for the alignment of the local director. The broken lines indicate the alignment of vectors pointing towards the centre, at all points around the circuit. Radial lines in the director field pattern occur at those α values where these two sets of lines intersect. For s = +1/2 this only occurs at the single radial line where $\alpha = 0^o$ (indicated by the blue squares on the left, and the blue line on the right).

3.3 Relationship between the α /ω plot and the brush patterns

Sketches of the director fields and the corresponding α/ω plots, for s values between -2 and +2 are shown in Figure 16. Nuclei with s values other than ±½ and ±1 are rarely encountered – but we have included them to help to illustrate the general relationship between s and the structures and optical properties of the nuclei.

Figure 16 about here

Figure 16
Plots of α against ω are used to explain the symmetry of director fields of nuclei with strengths ranging from +2 to -2.

In the plots in the left hand columns, the solid black lines indicate the ω values. The broken black lines indicate α values where the director points towards the centre of the nucleus. The places where these lines coincide, indicate the α values of the radial lines in the director field patterns. In the director-field diagrams shown on the right, radial lines are drawn in red. In the α/ω plots on the left, the corresponding coordinates are indicated by red circles.

The α/ω plot can be used to indicate the conditions for the formation of extinction brushes. These occur where the director lies parallel or perpendicular to the polariser, i.e. at 90^o intervals of ω, as shown in Figure 17.
In these plots, the black lines indicate ω values. The coordinates of α and ω where extinction occurs are indicated by red circles. The sketches on the right show the appearance of the brushes when the sample is viewed with vertical and horizontal crossed polars.

Figure 17 about here

Figure 17 Plots of α against ω used to explain the brush patterns for nuclei with strengths ranging from +2 to -2.
In the plots in the left hand column, the black lines indicate the ω values. Brushes occur at 90^o intervals of ω, where the director lies parallel or perpendicular to the polariser. The red circles indicate the values of α where extinction occurs. In the director field diagrams shown on the right, the brushes are indicated in the darker tone.

4. The rotation of brush patterns for rotating polars- and rotating-stage geometries

Section 3, above, dealt with the appearance of static situations (where neither the sample nor the crossed polars are rotated) and, as shown in figure (17) observations of the brush patterns in these cases will indicate the strength, but not the signs of the disclinations. However, the signs can be determined from the changes in the orientation of these brushes when either the sample or the crossed polars are rotated, using the two relationships given by Chadrasekhar in 1977 [7]. However, these were given with little exemplification and have been largely overlooked. Consequently the majority of the discussions given in current literature are either incomplete and confusing, or in some cases, incorrect. [12.13,14,15,16] .

With a conventional optical microscope, it is awkward to rotate the two polars synchronously, but the observations are simpler to interpret. Figure 18 shows this in the case of s = +½ . Here the rate of rotation of the brush pattern is twice that of the rate of rotation of the polars – and both rotate in the same sense. In general, the rate of rotation of the brushes is + 1/s times that of the sample, where the sign indicates whether the sense of rotation is the same or opposite.

Figure 18 about here

Figure 18 The relative rates of rotation of the brushes when the crossed polars are rotated, illustrated by the s = +1/2 case. In (a) both α and ω are 0^o. In (b) the crossed polars have been rotated by Rp = $+45^o$. This causes a rotation of the brush pattern (Rb) by 90^o - i.e. Rb/Rp = +2 .

The most common geometry used in the examination of optical textures is to keep the polars stationary and to rotate the stage. In this case the situation is one increment more complex to explain. As shown in Figure 19, the geometry of rotating the sample is, in a sense, the opposite to that of rotating the polars - and the resulting change in appearance of the brush pattern would be equal and opposite if the observer were to walk round the microscope at the same rate. However, for a stationary observer, the two situations are not directly comparable, and the rotation of the specimen with respect to the observer must be taken into account.
As an example, this figure shows how, for a +½ nucleus, a $+45^o$ rotation of the stage results in a -45^o rotation of the brushes.

Figure 19 about here

Figure 19 There are two ways in which a polarising microscopy study can be carried out - by rotation of the polars or by rotation of the stage.
In these sketches the broken lines indicate the initial alignment of the director in a particular region of the director field of the sample. To bring this region into extinction, either the polars can be rotated clockwise as shown on the left, or the sample can be rotated anticlockwise, by the same angle, as shown on the right.

However, the observed rotations of the brushes are not equal and opposite, because in one case the sample is rotating with respect to the observer and in the other case, it is stationary.

Chandrasekhar gives the general relationship $\omega = \alpha\,(s-1)/s$ for the way in which the brushes rotate as the sample is turned through an angle of α [7]. If this expression is recast as $\omega = \alpha\,(1 - 1/s)$, the second term corresponds to the rotation of the pattern with respect to the sample and the first term corresponds to the rotation of the sample with respect to the observer.

For a rotating specimen, in the case of s =+1, the brushes rotate with respect to the specimen at the same rate as the specimen, but in the opposite sense. The two effects cancel out, and the brush pattern remains stationary. Hartshorne states that the s = +1/2 nucleus was also of this "non-turning type" [15,16]. However, (as shown below), the brush pattern does indeed rotate.

Figure 20 about here

Figure 21 The rate of rotation of the brushes, as compared to the rotation of the stage, with stationary polars - as illustrated by the s = +1/2 case.
The upper figure shows the starting position with α and ω both at zero.
The lower figure shown the situation after a rotation of the stage by + 45°. The blue line (with gradient +1) shows the rotation of the stage. The black line (with gradient -2) shows the rotation of the brushes with respect to the stage. The green line (with gradient -1) corresponds to the resultant rotation of the brushes with respect to the observer.
Note that here, a +45° turn of the sample causes a -45° turn of the brushes – and, in general for the moving stage geometry, the rate of rotation of the bushes is a factor of (1 - 1/s) times that of the stage [7].

The results of rotating the six-brush nucleus shown in Figure 11 are plotted out in Figure 21. The measured average ratio of the angular velocity of the brushes to the angular velocity of the sample (Rb) is 0.32. For a +3/2 disclination, the expected value as given by Chandrasekhar's equation [7], is 1/3 (and for comparison, the calculated value for a -3/2 dislocation is 4/3).

Figure 21 about here

Figure 21 Analysis of the six-brush pattern.
This graph shows the change in orientation of a six-brush pattern as the stage is rotated (in 5^{o} increments) between stationary crossed polars. The orientation of each of the six brushes was measured separately. Six-brush patterns are given by disclinations of strength 3/2. The sign can be determined from the way in which the brush pattern rotates as the stage is turned. These data show that the ratio of angular velocities in this case is about 1: 3 - indicating a +3/2 disclination. For comparison, the ratio Rb for a -3/2 disclination would be 4/3 (see Figure 21 and Table 1).

In practice it is not always easy to estimate the value of Rb by eye, since the brushes do not have sharply defined edges and the shapes are distorted by the influence of neighbouring disclinations. Plotting a spread of data of this kind is recommended.

Accurate measurement of the orientation of a brush pattern is difficult. Brushes have no defined edges, and it is the alignment at the core of the nucleus which is to be measured - the pattern is progressively distorted in the outer regions by the influence of neighbouring disclinations.

Figure 22 about here

Figure 22 The relationship between the strength (s) of a nucleus and the relative rate of rotation of the brushes and the stage for the rotating polars geometry and the rotating specimen geometry. The trace for the rotating polars geometry (Rp =1/s) is shown in grey. Its inverse (-1/s) is shown in pink and the trace for the fixed polars geometry (Rs = (1 – 1/s) is shown in red. Note the loss of symmetry in the final spread of values.

Summary

Table 1

Strength s	Rot. sym	No. br (4|s|)	Rp (1/s)	Rs (1-1/s)
+2	2-fold	8	+1/2	+1/2
+3/2	1-fold	6	+2/3	+1/3
+1	(infinity)	4	+1	0
+1/2	1-fold	2	+2	-1
-1/2	3-fold	2	- 2	+3
-1	4-fold	4	-1	+2
-3/2	5-fold	6	- 2/3	+5/3
-2	6-fold	8	-1/2	+ 3/2

where: **Rot. Sym**. is the order of the rotational symmetry of the director field pattern
No. br is the number of brushes.
Rp is the ratio of the rate of rotation of the brushes and the rate of rotation of the crossed polars (with a fixed sample).
Rs is the ratio of the rate of rotation of the brushes and the rate of rotation of the stage (with fixed polars).

.

Table 1 shows the parameters discussed for all nuclei from s = +2 to s = -2. It indicates the symmetry of each nuclear pattern, the number of brushes and the way in which brush patterns rotate with s for both geometries. Note that no two nuclei with different values of s produce brush patterns which rotate at the same rates. In principle therefore, nuclei can be identified unequivocally by polarising microscopy.

Descriptions of the optics of nematic disclinations in current literature are often confusing and sometimes inaccurate. In particular, the distinction between the result of rotating the crossed polars (for a fixed specimen) and the result of rotating the specimen (with fixed polars) is not always made clear – and the two experimental geometries give different results.

We suggest that plotting data as an α/ω graph is a convenient way of recording the behaviour of brush patterns when viewed with a polarising microscope (especially when dealing with nuclei of higher s-values.

One of us (J. E. L.) would like to dedicate this paper to Norman Hartshorne, who in 1961, supervised the final year undergraduate project of an inept student fortunate enough to be assigned to him - and inculcated a lifelong love of optical microscopy.

Acknowledgements

E.I.L.J. acknowledges support in the form of an EPSRC studentship.

----------//----------

References

1 de Gennes PG, Prost J. The Physics of Liquid Crystals, Second edition, The International series of Monographs on Physics, Oxford Science Publications, Oxford University Press: 1993. ISBN 0-19-852024-7.

2 This dates back to 1890 when the German organic chemist, Ludwig Gatterman was examining a new compound he had made. This was para-azoxyanisole (PAA), destined to be the focus of investigations of the physical properties of the thermotropic nematic phase for the next half century. When viewed between crossed polars, his samples showed peculiar streaks which he called called S*hliere* (stains). Incidentally, Gatterman appears to have been the first person to have used the term *liquid crystals.*

See Page 25 of Dunmur D, Slukin T. Soap, Science and Flat-Screen TVs - A history of Liquid Crystals, University Press: 2011. ISBN 978-0-19-954940-5.

3 http://www.nobelprize.org/nobel_prizes/physics/laureates/2016/

4 Cladis P, Kleman M, Pieranski P. C.r. hebd. Sèan. Acad. Sci. Paris 1971; **B273:** 275. and reproduced in de Gennes, [1] in plates on un-numbered pages between pages 132 and 133),

5 Friedel J, Kleman M. Fundamental aspects of the theory of dislocations. Natn. Bur. Stand. spec. 970; **317** I: 607.

6 Kleeman M, and J. Friedel,J. J. Phys. (Fr.) **30,** (Suppl. C4): 1969. 43.

7. Chandrasekhar S. Liquid Crystals, Cambridge Monographs on Physics, Cambridge University Press. ISBN 0 521 21149. 1977; 2, ISBN 0521 29841 5.

8 Dierking I, Alexander GP, Yeomans JM. Phys. Rev. E 2012, **85** Issue: 2 Part 1 Article Number: 021703. DOI: 10.1103/PhysRevE.85.021703

9 Nikkhou M, Musevic M. Topological binding and elastic interactions of microspheres and fibres in a nematic liquid crystal. Eur.Phys. J. E, 2015 **38** Issue: 3 Article Number: 23 DOI: 10.1140/epje/i2015-15023-6.

10 Copar S, Tkalec U, Musevic I. Zumer,S. USA. Knot theory realizations in nematic colloids. USA, Proc. Nat. Acad. Sci, 2015; **112** Issue 6:1675-1680. DOI: 10.1073/pnas.1417178112

11 Musevic I. Light-controlled topological charge in a nematic liquid crystal. Nature Physics. **11 ;** 2015, Issue: 2:183-187. DOI: 10.1038/NPHYS3194

12 Elston S. Sambles R. Thermotropic Liquid Crystals, Taylor and Francis, 1998 ISBN-7484-0629-8s.

13 Dierking I. Textures of Liquid Crystals. 2004 Wiley-VCH Verlag GmbH & Co. KGaA, Print ISBN: 9783527307258, Online ISBN; 9783527602056 DOI: 10.1002/3527602054

14 Demus D, Richter L. Textures of Liquid Crystals, Verlag Chemie Weinheim, New York. 1978. ISBN 3-527-25796-9 (Weinheim) ISBN 0-89573-015-4 (New York.

15 Hartshorne N H. The microscopy of Liquid Crystals.1974 Microscope Publications Ltd, London, England Chicago, Illinois, ISBN-13: 978-0904962031, ISBN-10: 0904962032

16 An identical treatment of the above is given in Hartshorne NH, Stuart A. Crystals and the Polarising Microscope, 4th edn Arnold, London, 1970. ISBN-10: 0713122560 ISBN-13: 978-0713122565.

----------//----------

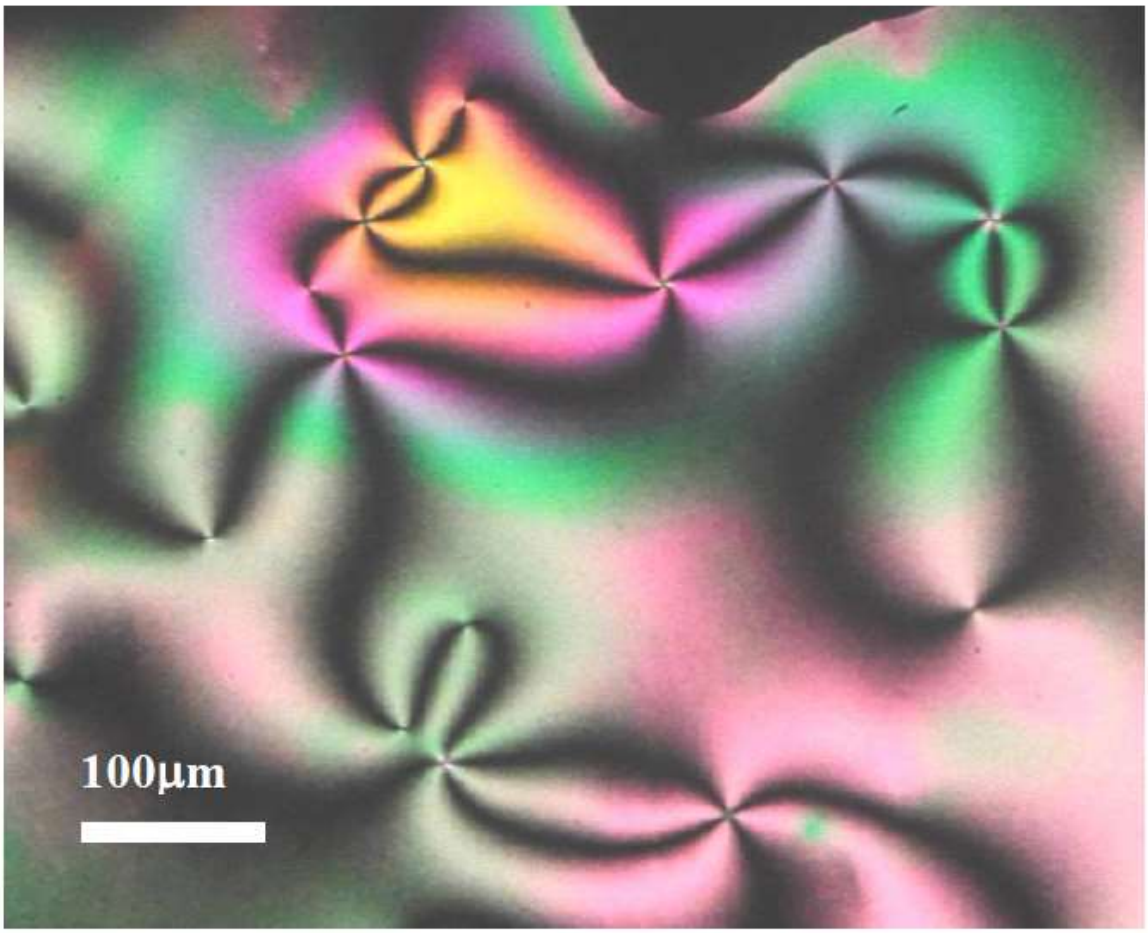

Figure 1

Figure 2

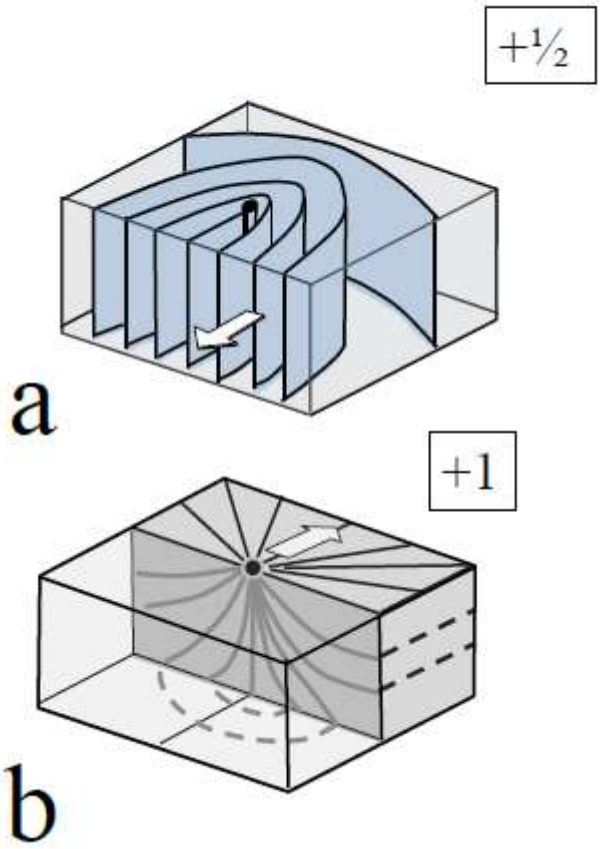

Figure 3

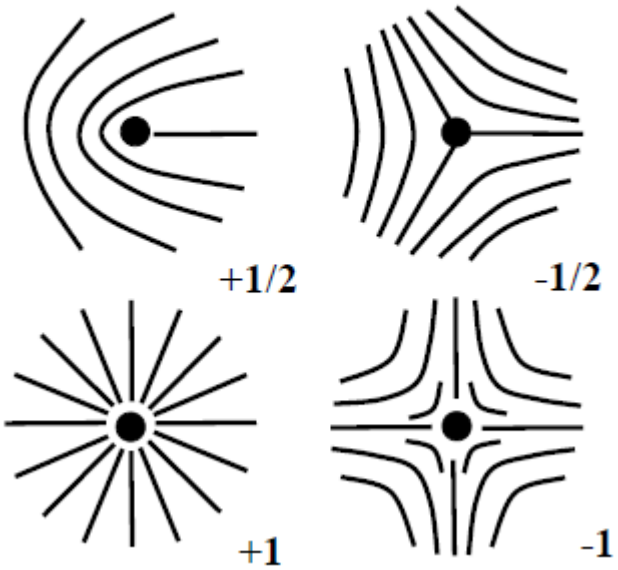

Figure 4

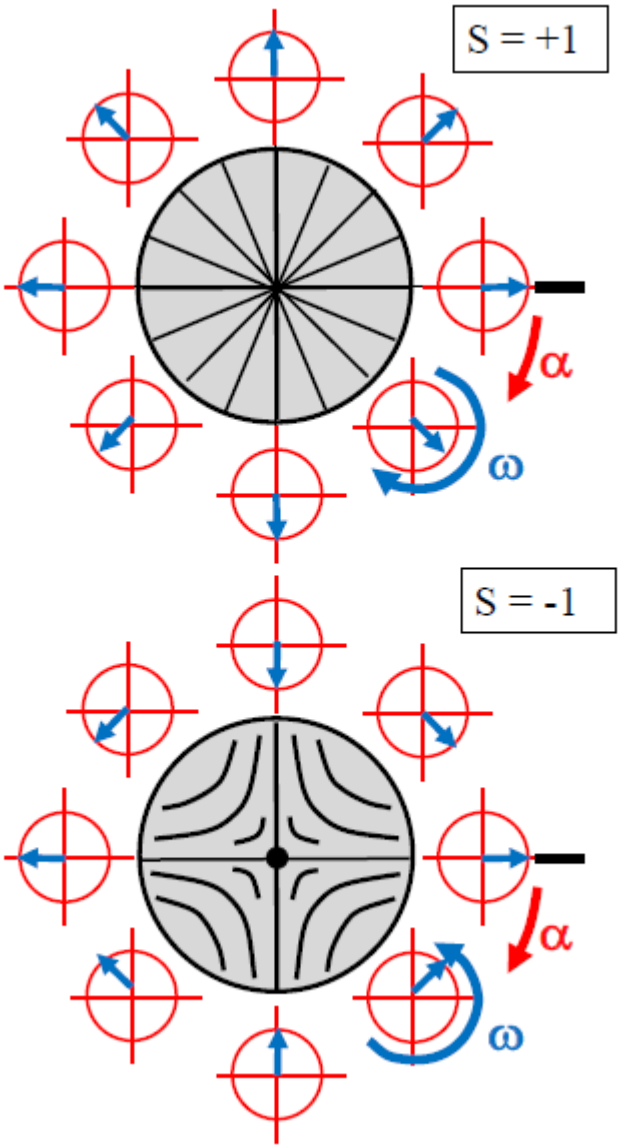

Figure 5

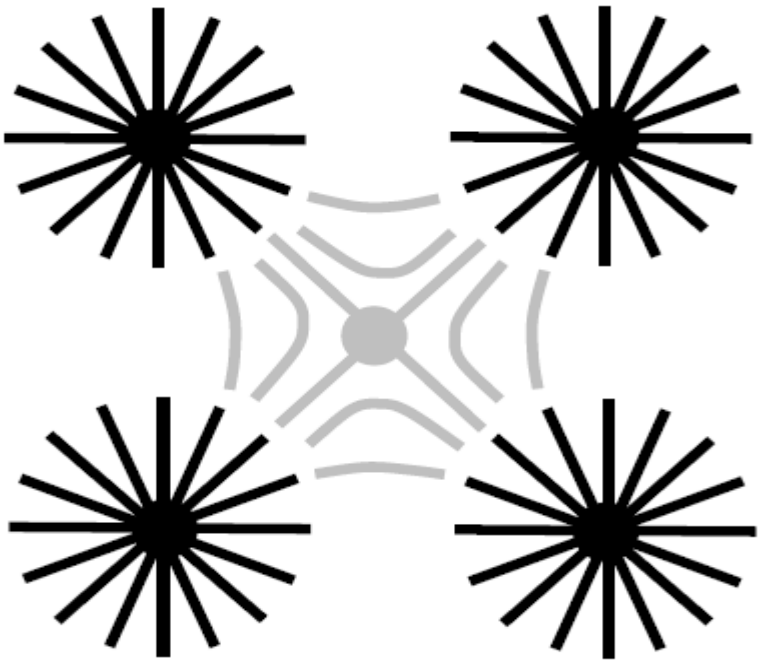

Figure 6

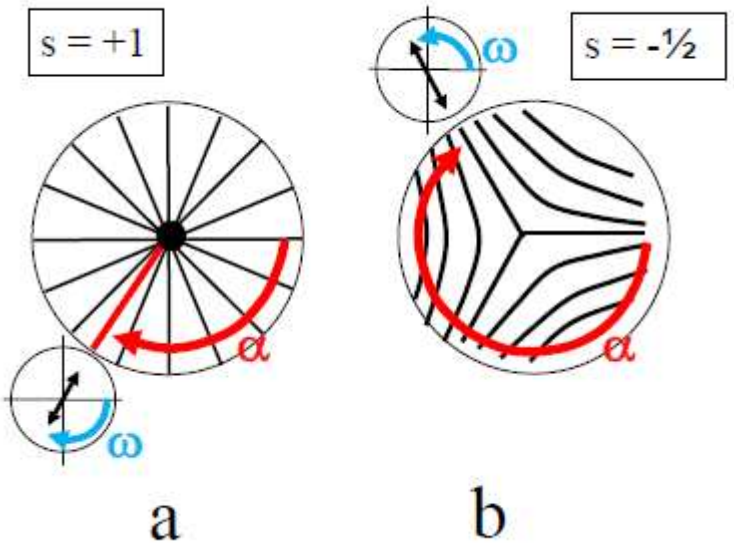

Figure 7

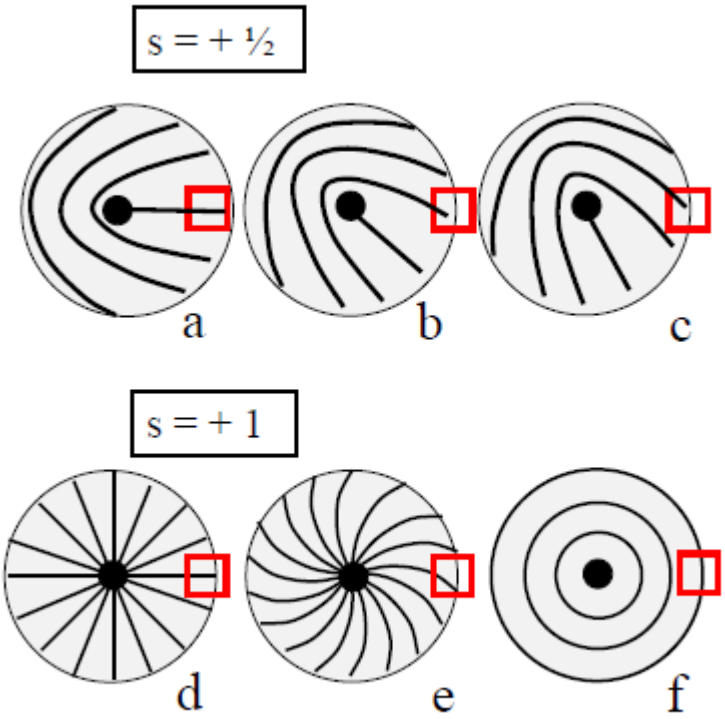

Figure 8

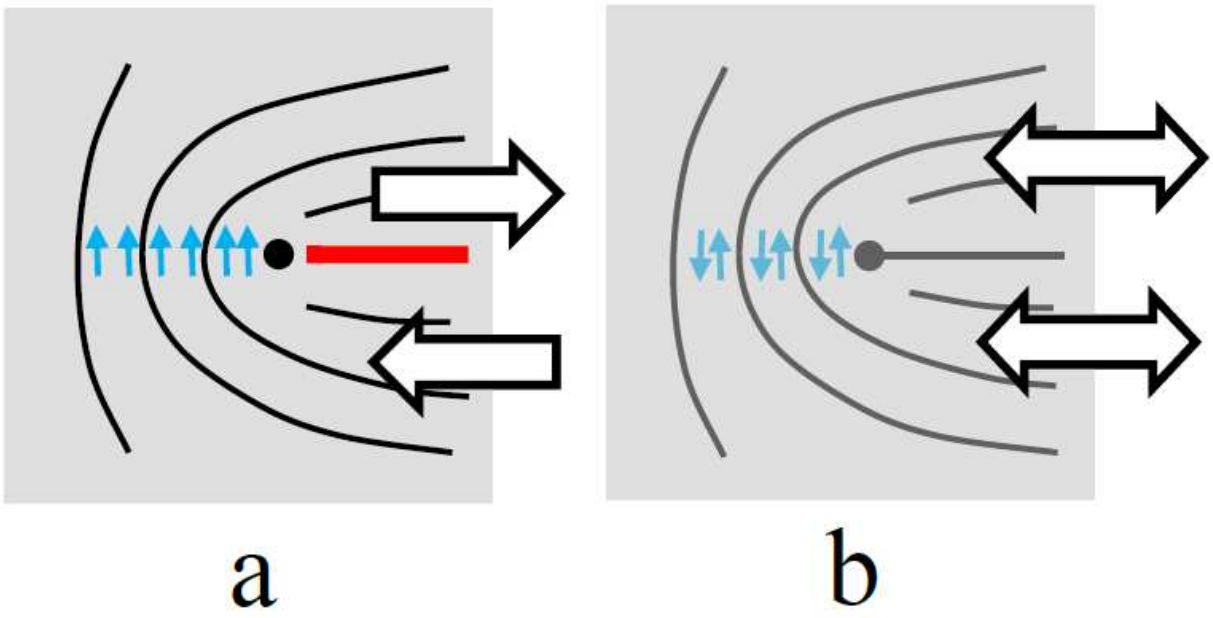

Figure 9

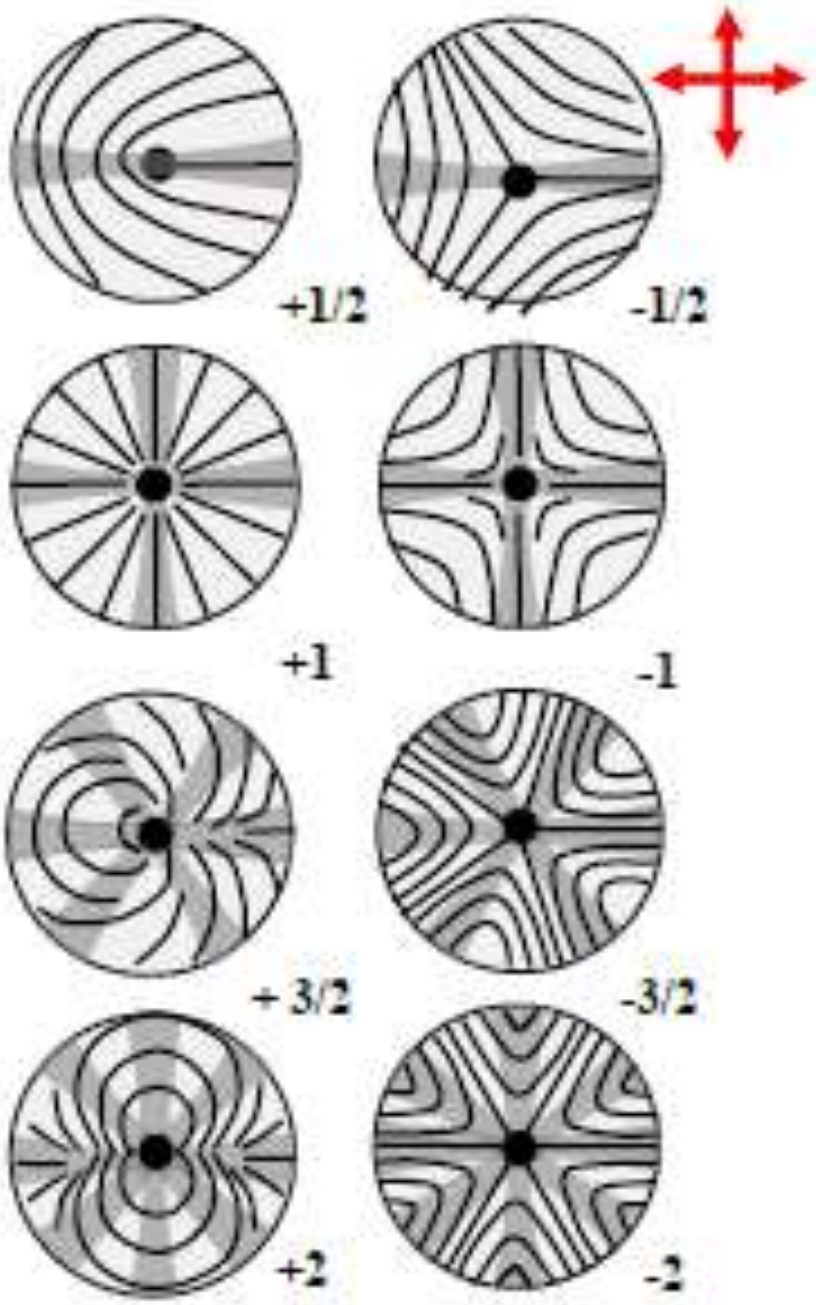

Figure 10

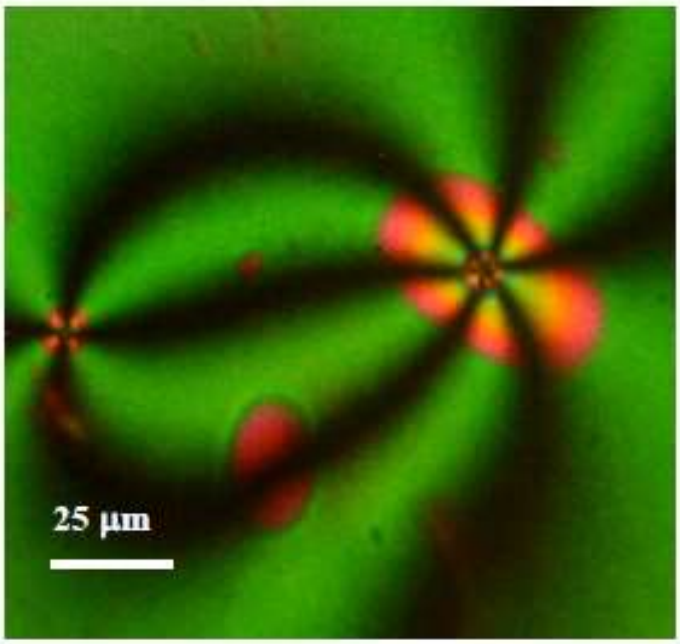

Figure 11

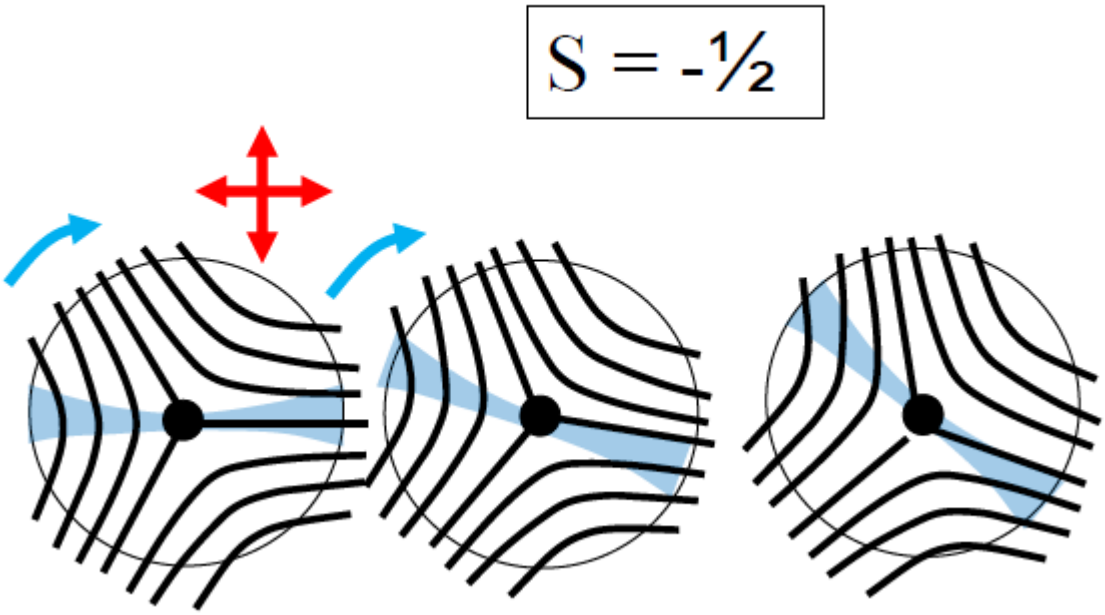

Figure 12

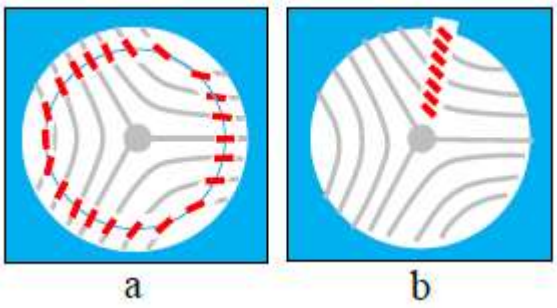

Figure 13

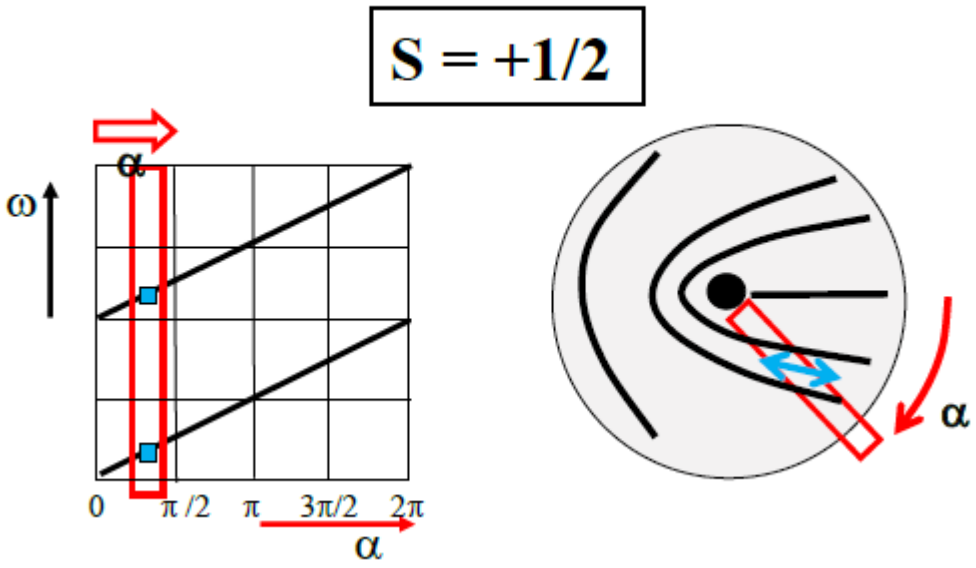

Figure 14

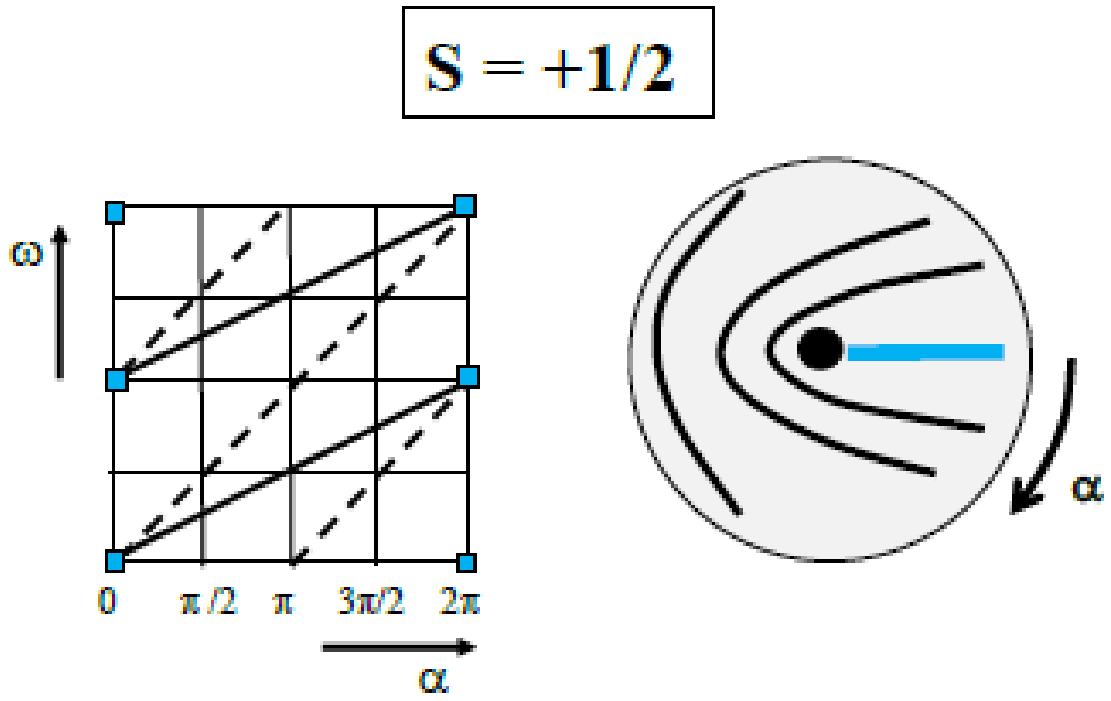

Figure 15

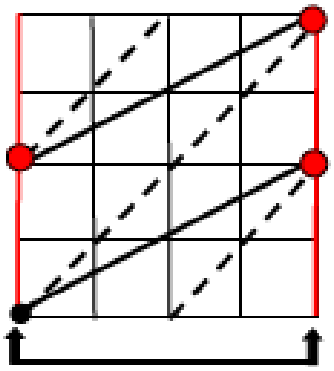

+1/2

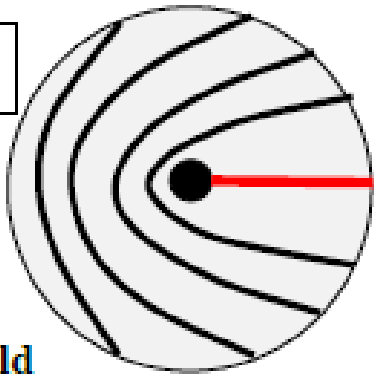

1-fold

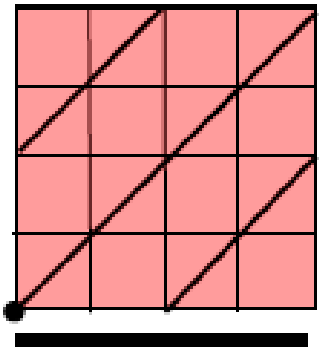

+1

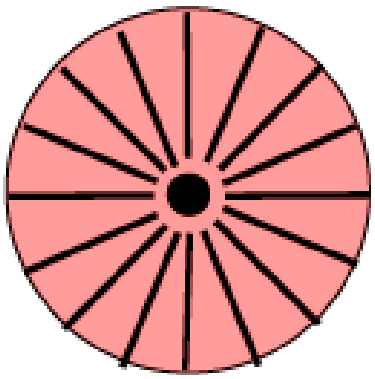

∞

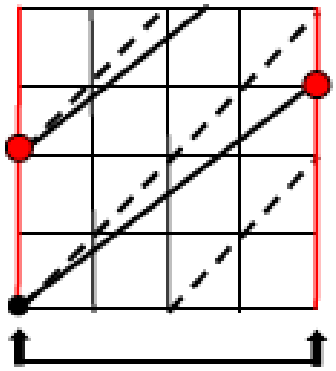

+ 3/2

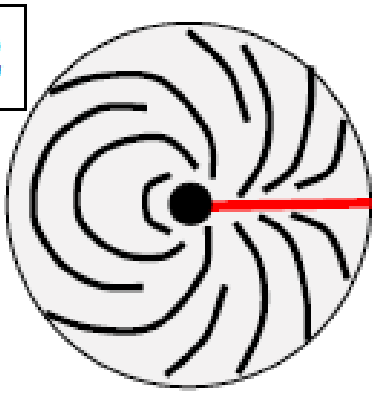

1-fold

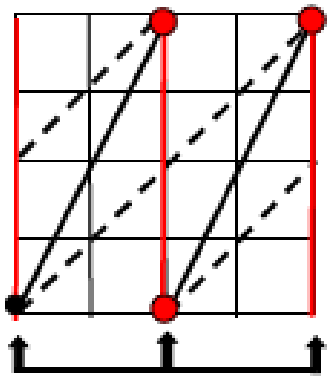

+2

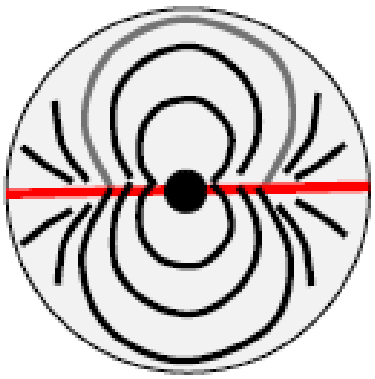

2-fold

Continued below

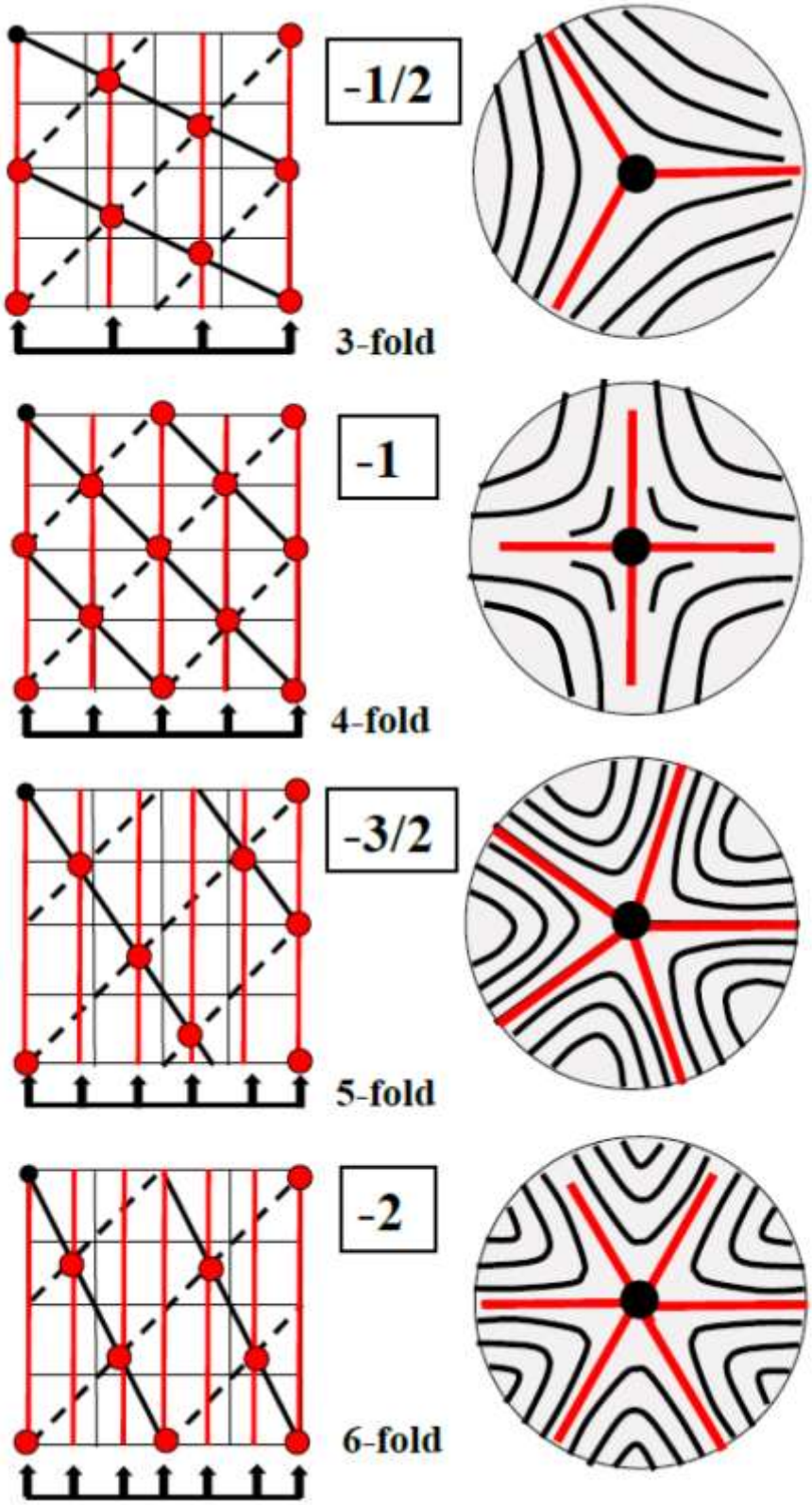

Figure 16

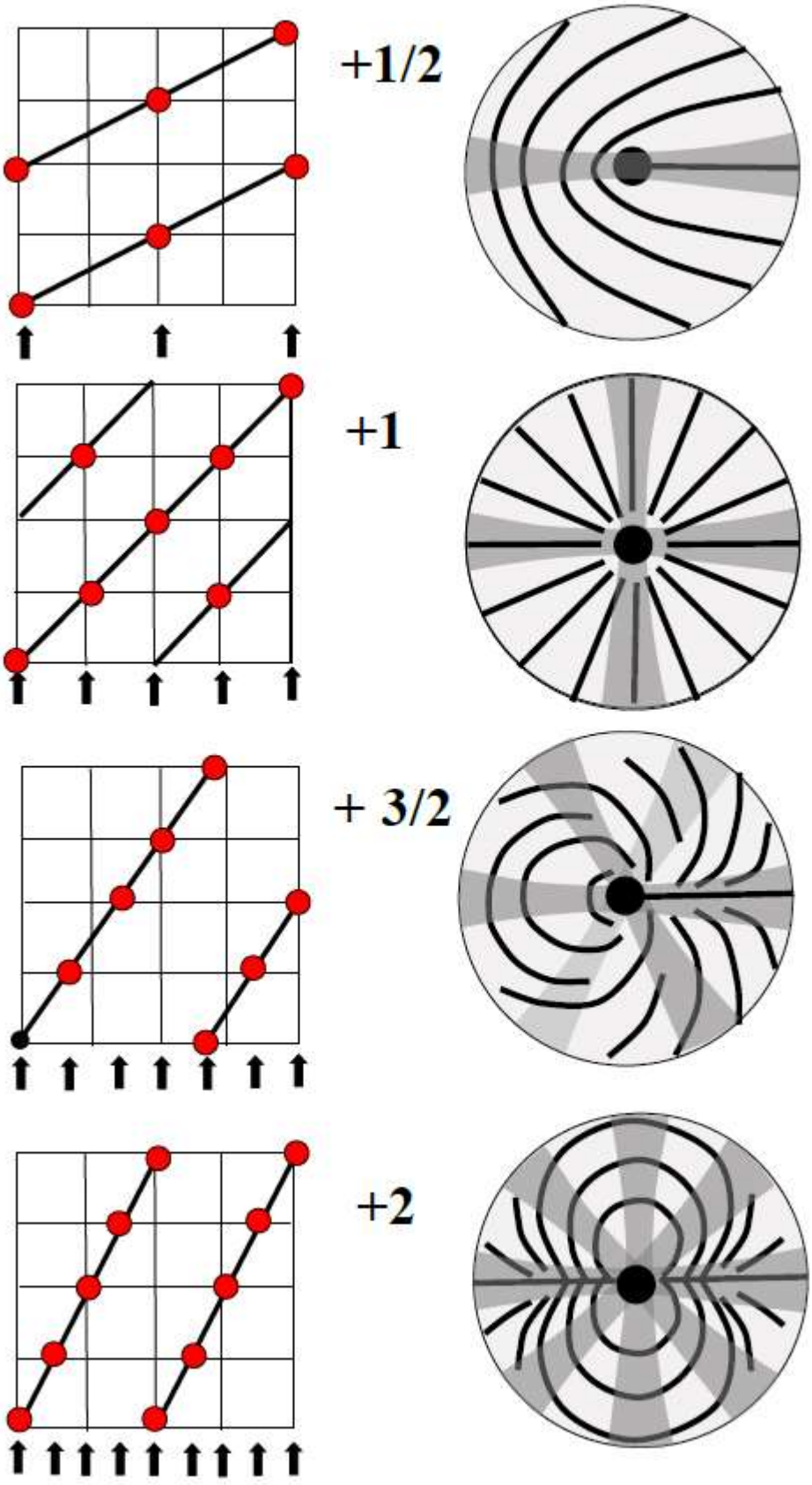
+1/2
+1
+ 3/2
+2

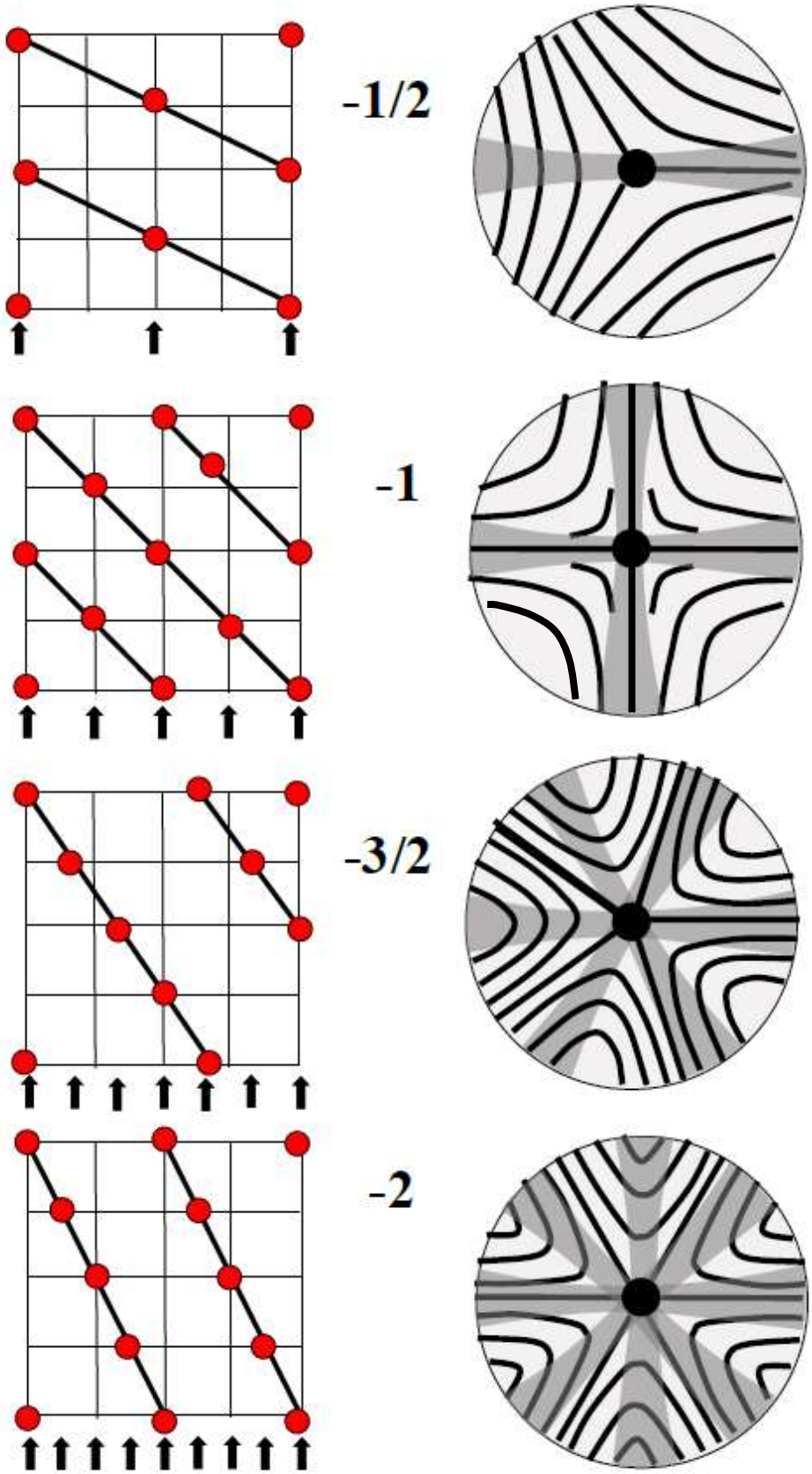

Figure 17

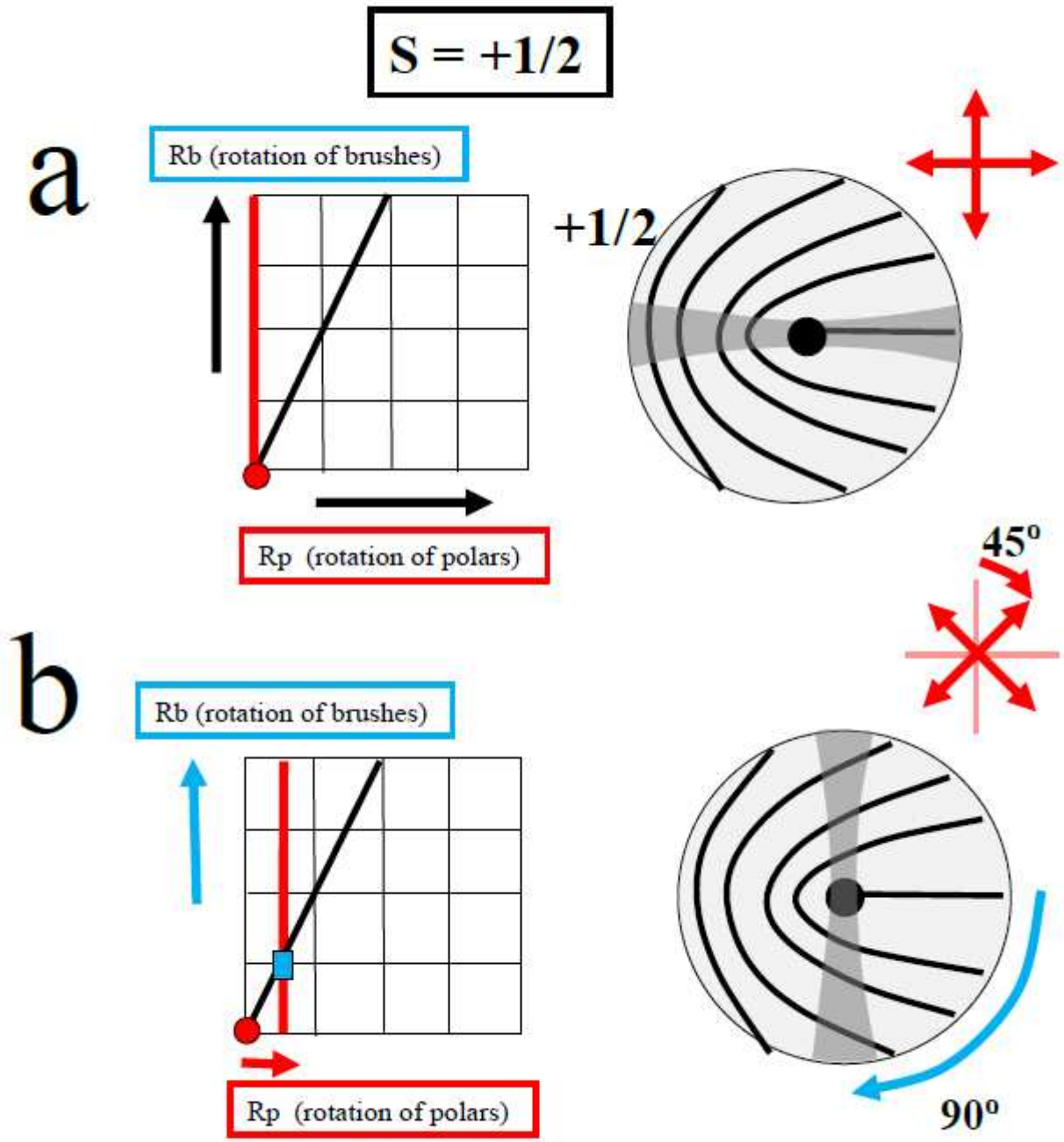
S = +1/2
a
Rb (rotation of brushes)
+1/2
Rp (rotation of polars)
45°
b
Rb (rotation of brushes)
Rp (rotation of polars)
90°

Figure 18

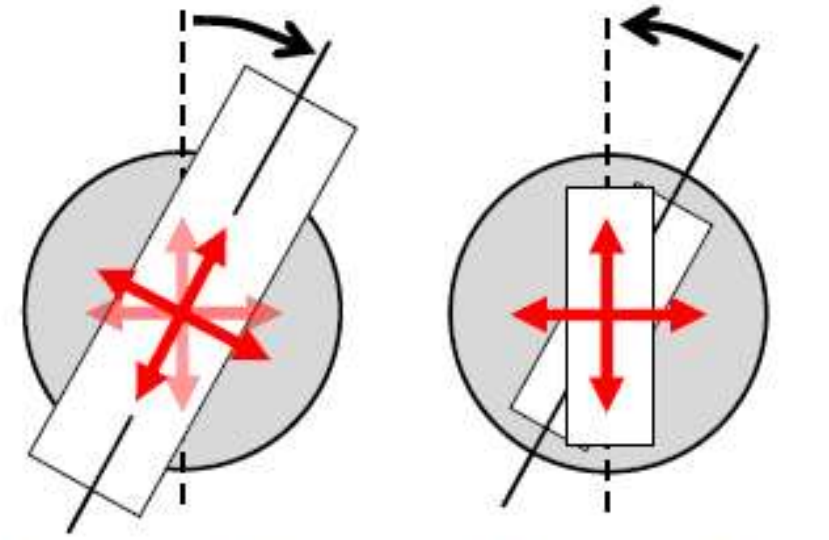

Figure 19

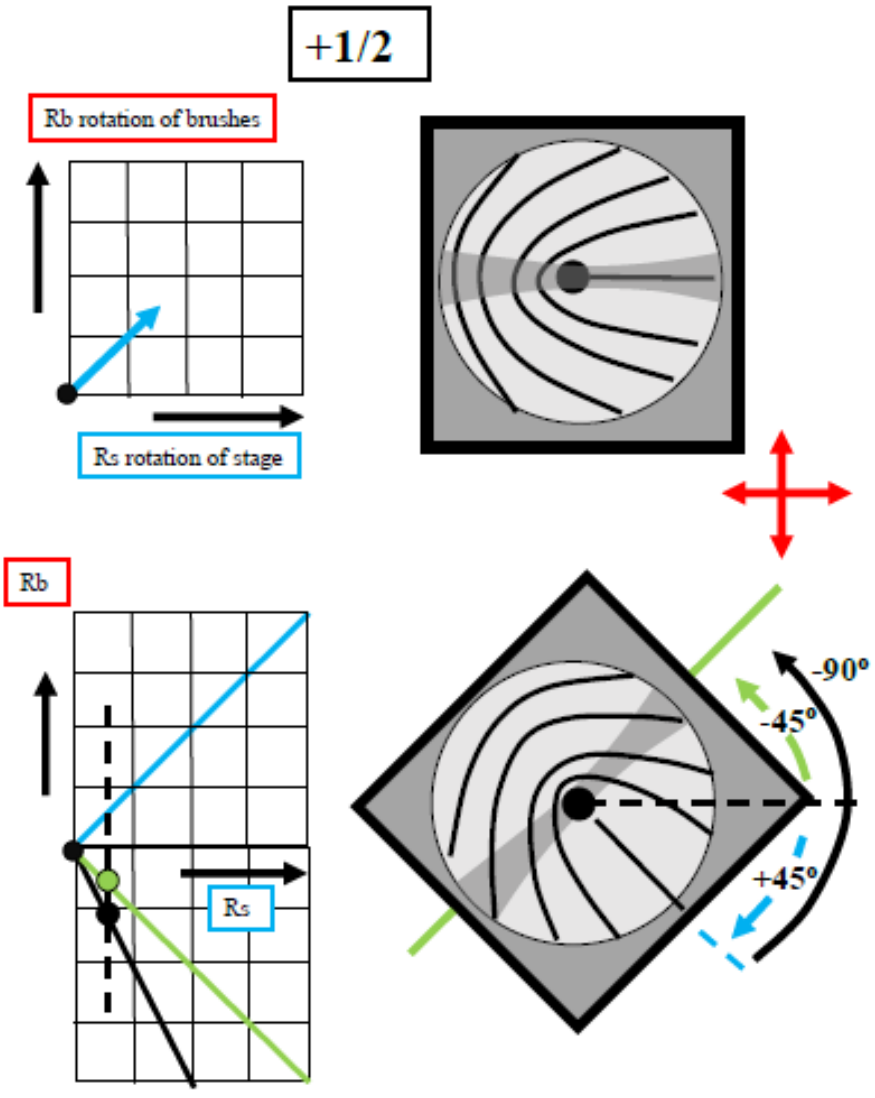

Figure 20

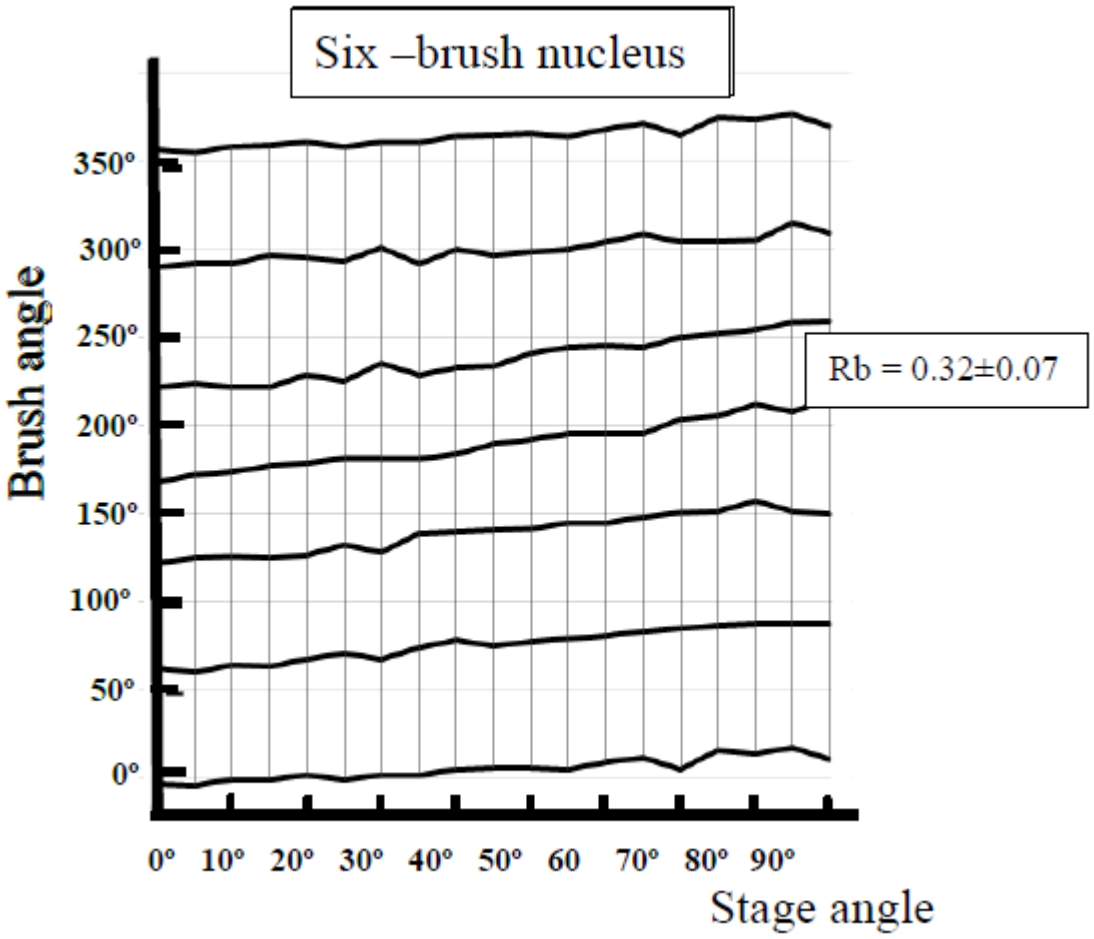
Six –brush nucleus
Brush angle
350°
300°
250°
200°
150°
100°
50°
0°
Rb = 0.32±0.07
0° 10° 20° 30° 40° 50° 60 70° 80° 90°
Stage angle

Figure 21

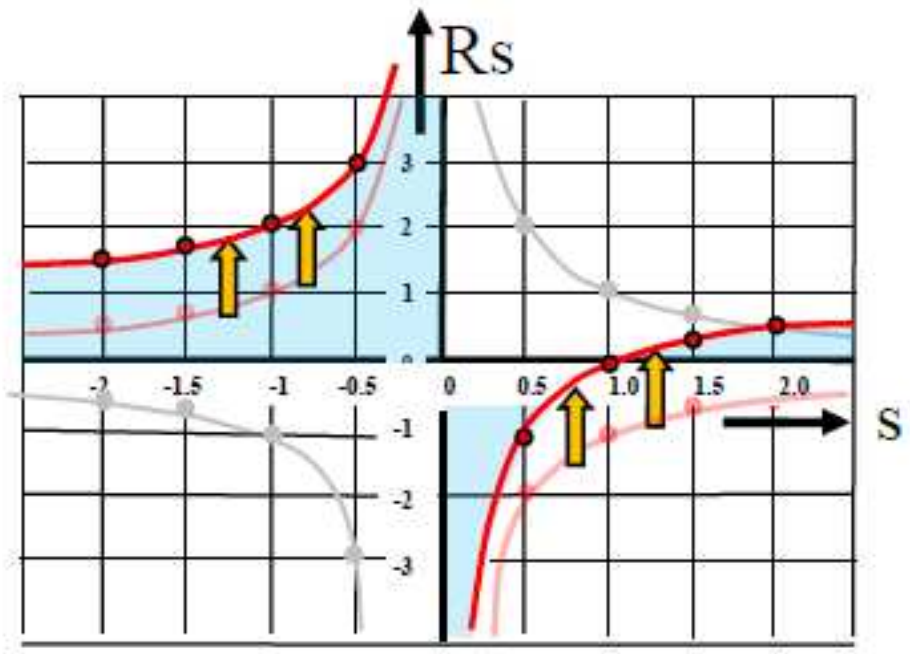

Figure 22